Kunert, Joachim; Ewers, Roland; Kleiner, Matthias; Henkenjohann, Nadine; Auer, Corinna

**Working Paper**

# Optimisation of the shear forming process by means of multivariate statistical methods

Technical Report, No. 2005,23

**Provided in Cooperation with:**
Collaborative Research Center 'Reduction of Complexity in Multivariate Data Structures' (SFB 475), University of Dortmund

*Suggested Citation:* Kunert, Joachim; Ewers, Roland; Kleiner, Matthias; Henkenjohann, Nadine; Auer, Corinna (2005) : Optimisation of the shear forming process by means of multivariate statistical methods, Technical Report, No. 2005,23, Universität Dortmund, Sonderforschungsbereich 475 - Komplexitätsreduktion in Multivariaten Datenstrukturen, Dortmund

This Version is available at:
https://hdl.handle.net/10419/22613

# Optimisation of the shear forming process by means of multivariate statistical methods

***Matthias Kleiner[1], Roland Ewers[1], Joachim Kunert[2], Nadine Henkenjohann[2], Corinna Auer[2]***

*[1]University of Dortmund, Department of Statistics*

*[2]University of Dortmund, Institute of Forming Technology and Lightweight Construction*

**Abstract**

*Shear forming is a versatile process for manufacturing complex lightweight components which are required in increasing numbers by many different industries. Inherent advantages of the process are simple tooling, low tool costs, good external and internal surface quality, close dimensional accuracy, and good mechanical properties of the components.*

*In times of free market economy, it is necessary to on the one hand fulfill the increasing demands toward the quality characteristics and on the other hand to reduce the development time needed to manufacture such a high quality component. Since shear forming is a complex and sensitive process in terms of deformation characteristics this is not an easy task.*

*To assess the overall quality of a component several, mutually contradictory, quality characteristics have to be considered simultaneously. While conventionally each characteristic is considered separately, in this paper, a statistical approach is presented which copes with the above mentioned demands and provides the opportunity for an efficient, multivariate optimisation of the process. With a minimum of statistically planned experiments, mathematical models are derived which describe the influence of the machine parameters and their interactions on quantitative as well as qualitative component characteristics. A multivariate optimisation procedure based on the concept of desirabilities is used to find the best compromise between the mutually contradictory quality characteristics.*

*With this statistical approach a workpiece for electrical industry is manufactured which requires a very good surface quality and close geometrical tolerances.*

**Keywords:** Shear forming, experimental design, multivariate optimisation, high voltage divider

## 1. Introduction

Shear forming, also called power-spinning or spin-forging, is a derivative of metal spinning. It is a competitive production technique enabling conical, rotationally symmetrical components to be produced to extremely close tolerances. By shear forming a circular blank is formed incrementally to hollow bodies by a roller tool which forces the blank onto a mandrel. Figure 1 gives a schematic overview of the shear forming process. The blank is clamped centrically against the mandrel by means of a tailstock. When the complete assembly is rotated the blank is formed continuously by the CNC-controlled roller tool which moves in one single pass parallel to the contour of the mandrel. The shear forming process can only be used for conical workpieces and the profile shape of the component has to be inclined between an angle of above 10° to 18° and below 80°, depending on the material used. The contour can be of linear, concave or convex nature. For more complex workpieces, different geometries are usually combined. Typical components formed by shear forming are, for example, funnels, lamp housings, reflectors, tank ends or music instruments. Some examples of shear formed workpieces are shown in Figure 2. The resulting wall thickness in shear forming is predefined by the cone angle of the contour and achieved by controlling the gap between the roller and the mandrel so that the material is displaced only axially, parallel to the axis of rotation. The required reduction of the wall thickness is described by the sine law which states that the wall thickness of a spun component is equal to the wall thickness of the blank multiplied by the sine of the half apex angle of the cone, $\sin\alpha$. Due to this law, the smaller the apex angle of the cone is chosen, the higher the percentage reduction of the wall thickness of the blank and the greater the degree of forming required.

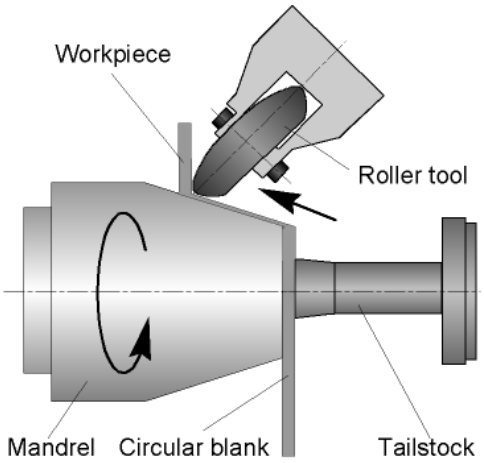


Fig. 1. Principle of shear forming

Fig. 2. Typical workpieces of shear forming, see Ott [1]

In the study presented here, preforms for the heads of a high voltage divider are produced in cooperation with the company Poynting GmbH, Germany. The HV-divider is used in high voltage technology to reduce an incoming voltage to a defined level. It consists of two conductive heads made of pure aluminium AA-1050A (Al99,5 w7). These heads are mounted in a defined, adjustable distance by a non conductive cylinder, see Fig. 3. This workpiece is used in air or oil environment. The demands toward the component were clearly set by the electrical properties of the workpiece. The desired geometry of the component was specified by a starting diameter of 90 mm, a cone angle of 42° degree, a wall-thickness of 1.34 mm and a height of the component of 54 mm, see Figure 4. The most important quality characteristic is the inner and outer surface quality. If this quality characteristic is not fulfilled, by using voltages of about 150KV the surface roughness may cause sparking. To prevent this phenomenon, additionally to the good surface quality all radii have to be very smooth without any edges.

Fig. 3. Examples of high voltage dividers

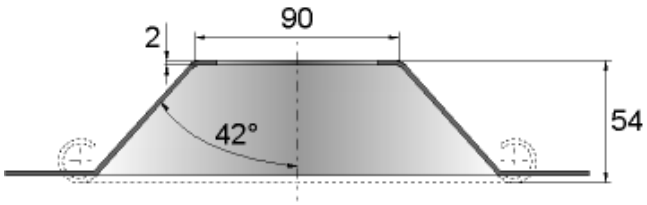


Fig. 4. Section of pre-form and contour of the final workpiece

Theoretical and experimental investigations of the shear forming process have been carried out for a long time. An overview of developments in terms of research and industrial applications for the shear forming process is given for example in Wong et al. [2] or Smith [3]. A theoretical analysis of the shear forming process has been carried out by, for example, Kalpakcioglu [4], Avitzur et al. [5, 6], Kobayashi et al. [7, 8], Slater and Joorabchian [9] and Hayama [10, 11]. In the focus of these investigations are mainly models to describe and predict the occurring forming forces as well as models for the prediction of instabilities of the process as for example the wrinkling of the flange. Despite the fact that these theoretical descriptions gave a basic insight into the process, the models are only a rough description of the manifold effects occurring during the forming process and ,hence, have only limited relevance for practical application. Actual developments scope on a better understanding of the process by simulation, see for example Dan et al. [12] or Kim et al. [13]. Unfortunately, due to the incremental forming process the models are very difficult and simulation is still very time consuming. Due to this, the theoretical investigations have been completed by several experimental investigations, especially by Hayama et al. [14, 15, 16, 17], as well as, for example, Murata and Ohara [18], Slater and Joorabchian [19] and Chen et al. [20, 21]. In the focus of these investigations is mainly the influence of single process parameters

on different characteristics of the process as well as the spinning forces. Important characteristics considered were process limitations as instabilities of the flange and fractures of the wall as well as quality characteristics like the surface roughness, and geometrical deviations. Many of these published articles focus on the variation of a single factor while keeping the other factors fixed. The major disadvantage of this so-called One-Factor-at-a-Time (OFAT) strategy is that possible interactions between the factors can not be considered. By employing statistical design of experiments and regression models Chen et al. [20, 21] solve this problem. The derived univariate models describe the relationship of several machine factors and their interactions on the surface quality at the in- and outside of a spun component and on the spinning force. Verification runs showed that these models allowed a reasonably good approximation of the true underlying relationship.
In order to asses the overall quality of a spun component, several quality characteristics have to be considered simultaneously. In the study presented here, primary attention is focused on the surface quality at the inside and outside. But additionally, the geometry of the component should not be disregarded. By the approach presented by Chen et al. [20, 21], the shear forming process can only be optimised for each quality characteristic separately. But the investigations described above have shown that responses tend to mutually contradict each other in the sense that when a machine parameter setting is changed to improve the quality of one response, the quality of another response is reduced. Hence, in order to guarantee an overall quality optimisation of a component, it is necessary to apply a method which guarantees to find the best compromise between the responses. In this paper, a suitable multivariate optimisation procedure is presented. This method is applied to produce a high voltage divider fulfilling the requirements made toward the quality characteristics. In section 2, the statistical methods used are briefly described. The experimental setup is explained in section 3. Univariate models of the individual responses are derived and interpreted in section 4. Additionally, the results of the multivariate optimisation are presented. Finally, a short summary is given in section 5.

## 2. Statistical methods

In this section, a brief overview of the statistical methods used in this study is given. Statistical experimental designs are a powerful tool to obtain, with a minimum number of experiments, a maximum of information about the underlying process. In section 2.1, the construction and analysis of mixed level designs, which are not that common, is briefly presented. Based on the experimental data, mathematical models can then be fitted which describe the influence of the machine parameters and their interactions on the quality characteristics. In section 2.2, a suitable model for qualitative responses is presented. Finally, in section 2.3 a multivariate optimisation technique is presented to cope with quality characteristics which conflict each other.

### 2.1 Construction and Analysis of Mixed Level Designs

In order to asses the influence of several factors on a response, a frequently used strategy of experimentation is the One-Factor-at-a-Time-Method. As the name indicates, in each step of the experiment only one factor is varied. In classical design of experiment (DoE) several factors are varied simultaneously. DoE, in contrast to OFAT, allows to identify and to interpret interactions between the factors. Fractional factorial designs and central composite designs are two of the most popular statistical designs, see Montgomery [22]. But these designs impose the number of factor levels in the design to be equal. In some situations it is not possible or sensible to observe an equal number of factor levels. When analysing the shear forming process we were confronted with this problem. A class of designs which copes with such data structures are mixed level designs. One method to construct mixed level designs is to use so called product arrays of fractional factorials of different number of levels. For each run of a fractional factorial with $k_1$ levels the whole other fractional factorial with $k_2$ levels is run. However, this often leads to a design with an unacceptable high number of runs. More efficient methods, namely the method of replacement and the method of collapsing factors, are proposed by Addelman [23, 24]. These methods are explained briefly in the following.
The basis of such a design is an appropriate fractional factorial, where each column presents a factor. For the method of collapsing factors, in the first step a fractional factorial with s levels is constructed. In the next step, either a factor with $s$ levels is collapsed to a factor with only $t$ levels, where $t<s$. Or

alternatively, the factor with *s* levels is collapsed to (*s*-1)/(*t*-1) factors each with *t* levels, where *s* is a power of *t* and *t* is a prime or the power of a prime.
In the main, the method of replacement is the reverse of the method of collapsing factors. The basis is a fractional factorial with t levels. Using the method of replacement (*s*-1)/(*t*-1) factors each having *t* levels are replaced by one *s*-level factor, where *s* is a power of *t* and *t* is a prime or the power of a prime.
To illustrate the construction of mixed level designs, the correspondence scheme in Table 1 shows how to get a three-level factor X from two two-level factors A and B and their interaction AB by using the method of replacement and the method of collapsing factors.
Addelman proposes to analyse the data of a mixed level design according to the theory of linear models as described in the next section.

Table 1
Correspondence scheme

| **Two-level factors** | | | **Replacement** | **Four-level factor** | **Collapsing** | **Three-level factor X** |
|---|---|---|---|---|---|---|
| **A** | **B** | **AB** | | | | |
| -1 | -1 | 1 | → | 0 | → | -1 |
| -1 | 1 | -1 | → | 1 | → | 0 |
| 1 | -1 | -1 | → | 2 | → | 0 |
| 1 | 1 | 1 | → | 3 | → | 1 |

### 2.2 Proportional Odds Models

Whereas quantitative response variables can be fitted by classical regression models, see Montgomery [22], qualitative responses require a special class of models. A reasonable model for this situation is the so-called proportional odds model which is a generalization of the logistic regression model. This model assumes the existence of an underlying continuous response variable *Y**. But instead of *Y** only the categorical variable *Y* can be observed. The expected value of *Y** changes depending on the setting of the factors. Let a fixed parameter setting of the factors be denoted by x, and $P(Y \le j \mid x)$ the cumulative probability that the response *Y* falls into a category $\le j$ for a given *x*. The proportional odds model is then defined by

$$\ln \frac{P(Y \le j \mid x)}{1 - P(Y \le j \mid x)} = \alpha_j - \beta' x \,.$$

In terms of probabilities the proportional odds model can be converted to

$$P(Y \le j \mid x) = \frac{\exp(\alpha_j - \beta' x)}{1 + \exp(\alpha_j - \beta' x)},$$

where $\beta$ is the parameter vector and $\alpha_j$ are the so called cut points. These correspond to the values of *Y**, that divide the categories *j* and *j+1* of *Y*. The model parameters are estimated by the maximum likelihood method. For a fixed parameter setting, this model allows to predict the probability of the response *Y* to fall in a certain category. In praxis, usually the category with the highest probability of occurrence is considered. A detailed description of the model can be found in Agresti [25].

### 2.3 Multivariate Optimisation with Desirabilities

A common approach for multivariate optimisation is to combine the response variables into a single response variable, which can then be optimised univariatly. One reasonable possibility to combine the response variables is based on the concept of desirabilities as proposed by Derringer and Suich [26]. Each response variable $y_i$ is transformed into a desirability $d_i$, which is a scale-free variable taking values between 0 and 1. The desirability is chosen so that it is zero when the response variable is outside its specification limits. A desirability of 1 is observed when the response variable is at its target $\tau_i$. The

general definition of the desirability for a nominal the best (NTB) variable $y_{ij}$ for response *i, i=1,..., I,* at run *j, j=1, …, J,* is given by

$$d_{ij} = \begin{cases} 0, & y_{ij} \le LSL_i \\ \left( \dfrac{y_{ij} - LSL_i}{\tau_i - LSL_i} \right)^l & LSL_i < y_{ij} < \tau_i \\ 1, & y_{ij} = \tau_i \\ \left( \dfrac{USL_i - y_{ij}}{USL_i - \tau_i} \right)^r & \tau_i < y_{ij} < USL_i \\ 0 & y_{ij} \ge USL_i \end{cases}$$

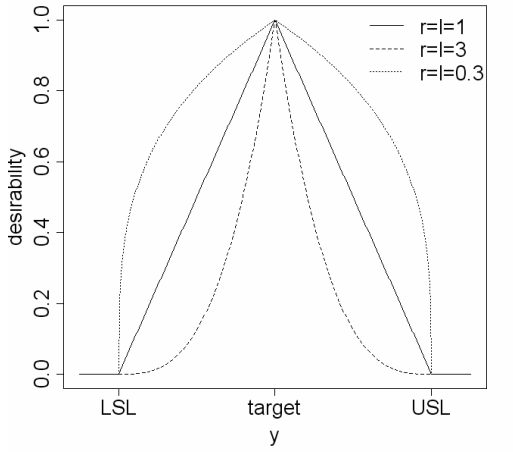


Fig. 5. Desirabilities for varies values of *r* and *l*

where the exponents *r* and *l* are chosen according to the importance of $y_i$ being close to $\tau_i$ . A convex shape is obtained for values of *r* and *l* larger than 1, and a concave shape for values of *r* and *l* smaller than 1. The parameters $LSL_i$ and $USL_i$ define the lower and upper specification limit for response variable $y_i$, respectively. $LSL_i$, $USL_i$ and $\tau_i$ have to be defined according to technical considerations. Some typical desirability functions for different values of *r* and *l* are shown in Figure 5. If deviations from the target value are considered to be more severe in one direction than in the other, different values of *r* and *l* have to be chosen. Definitions for the desirabilities of smaller and larger the best (STB and LTB) characteristics are analogous and can be found in Derringer and Suich [23]. The individual desirabilities can then be combined to an overall desirability $OD_j$ for each run j by computing the weighted geometric mean $OD_j = \prod_{i=1}^{I} d_{ij}^{w_i}$ , *j=1,…, J,* where $w_i$ denotes the weighting of the individual response as specified by the user. This overall desirability has the property of being zero, as soon as one individual desirability takes this value. Hence, if one of the responses is out of its specification limits the overall desirability is zero. By this approach, it is possible to identify the parameter setting of the factors which guarantees the best compromise between mutually contradicting responses.

## 3. Experimental setup

The experiments were conducted on a Leifeld spinning machine of the type APED 350 NC with a Sinumeric 840d CNC-control-unit. Corresponding to the workpiece geometry, circular blanks were used with a sheet thickness of t = 2 mm and an outer diameter of $D_0$ = 260 mm. The material used was pure aluminium AA-1050A, with a hardness of about 20 HB. Before each run, on both sides of the blank lubricant oil with low viscosity of type Castrol Illuform PN 226 has been applied to reduce friction and to improve the surface quality of the components, see also Hayama [17]. The spinning mandrel is made of low carbon steel with a surface quality of $R_z < 2.5$ µm.

### 3.1 Process parameters

The most important process parameters influencing the quality of the component are the clearance between mandrel and roller tool, the roller head radius, roller feed, mandrel revolution, original thickness of the blank, material type and cone angle of the mandrel. Since cone angle, the material type, and the diameter and thickness of the blank are specified by the demands of the user, these factors will not be varied. All the other process parameters are considered in this study.
In our investigations, we have used different roller tools with a diameter of $D_{DW}$ = 200 mm and a head-radius varied between $R_{DW}$ = 10 mm and $R_{DW}$ = 20 mm. The material of the roller tools is hardened, cold

working steel. This material has a very smooth, polished surface with $R_z < 0.4$ µm. The main reason for using such large head-radii is the achievement of a good surface quality. The positive effect of a large head-radius on the outside surface quality is obvious and has been confirmed within the investigations of for example Chen et al. [20]. Within the experimental and theoretical investigations described above, the effect of the head-radius on the spinnability seems to be low, see Kalpakcioglu [4]. Hayama et al. [14] point out that the flange deformation is scarcely affected by the head-radius of the roller tool and Hayama and Tago [15] show that it influences the occurrence of cracks only in an indirect way. By increasing the head-radius the critical feed-rate $\kappa$ = feed (f) / spindle speed (n) is reduced a little bit. On the other hand a large head-radius has a negative effect on the spinning forces and on the geometrical accuracy. As shown in Avitzur and Yang [6], a bigger value of $R_{DW}$ increases the frictional forces in the contact area between roller-tool and blank and by this especially the tangential force. As well known from flowforming, this leads to an undesired tangential flow of the material resulting in an increase of the workpiece-diameter. Due to this, a process set-up has to be found that compensates this effect.
Despite the fact, that the clearance is given by the sine law, it is important to include the gap distance as an influencing factor into the experimental setup, because the machine is not absolutely rigid due to the large forming-forces. As a consequence, the theoretical optimum for the gap distance differs slightly from the practical one. For the high voltage divider, the theoretical optimum, calculated by the sine law, is 2 mm*sin(42°)=1.338 mm.
Additionally, the elasticity of the material results in a significant amount of springback, resulting in an increasing geometrical deviation for an increasing height of the workpiece. Hence, in order to guarantee a spun component with a cone angle as exact as possible, this effect has to be compensated. Beneath an improved geometry of the roller tool or an adaptation of the geometry of the mandrel, one possible solution is to programme a linear tool path which slightly declines towards the end of the production process, as visualized in Figure 6.

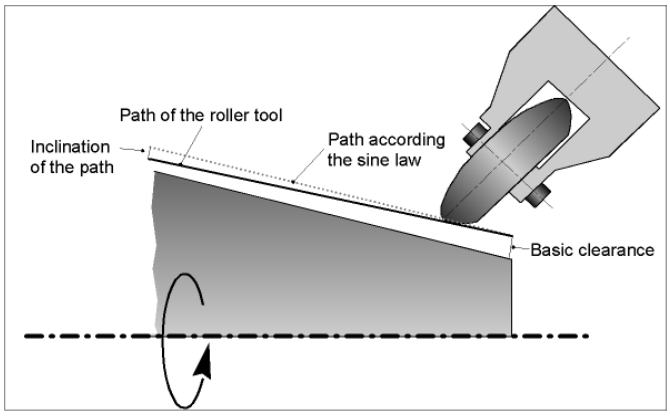

Fig. 6. Inclination of tool path

The negative side effect is that if the inclination is set too large, no constant wall thickness can be produced and the occurrence of instabilities is increased. Due to the sine law and the effects discussed above, for the factor “gap distance” an optimum exists and hence it is reasonable to consider deviations from this optimum in both directions. For the considered inclination of the tool path also three factor levels will be observed to allow a better assessment of this factor. As a consequence, in the experimental design these two factors are considered at three levels. For the other factors, roller head-radius, roller tool feed and mandrel revolution, two levels are observed. In Table 3, the observed factor levels are shown.

Table 3
Factor levels of the machine parameters

| **Factor** | **Low** | **intermediate** | **high** |
|---|---|---|---|
| Roller tool radius | 10mm | | 20 mm |
| Roller tool feed | 400 mm/min | | 800 mm/min |
| Mandrel revolution | 800 1/min | | 1200 1/min |
| Distance of gap | 1.138 mm | 1.338 mm | 1.538 mm |
| Inclination of tool path | -0.1 mm | 0 mm | 0.1 mm |

### 3.2 Response variables

In order to assess the overall quality of a component several quality characteristics were observed. The observed responses can be divided in two groups. The first group of responses measures deviations from the desired geometry and the second the surface quality of the component. In the first group, next to the cone angle of the final workpiece, the flange angle of the component is considered. It measures the deviation of the flange from the theoretical optimum of 90° degree. This characteristic is important for the subsequent forming of the end radius, as shown in Fig. 3 and Fig. 4. Furthermore, the material thickness is measured at six equally spaced heights of the component.
The surface quality is observed at the in- and outside of the component. In contrast to other experimental studies like for example Chen et al. [20, 21] the surface quality was not measured by the surface roughness criteria $R_a$ and $R_z$. Instead, qualitative scales were chosen to distinguish the inside-surface quality with respect to formations of rills und so-called dimpled skin. Dimpled skin results from slip-bands remaining at the surface due to a loss of contact between mandrel and inner surface of the workpiece. The six categories chosen for the inner surface quality are given in Table 2. The difference between dimpled skin and rills is shown in Figure 7. Since at the outside surface of a component the phenomenon of dimpled skin does not occur due to the contact with the roller tool, for this factor seven categories were chosen. The smaller the category number, the better the outside surface quality of the component. Mechanical engineers experienced in shear forming allocated the components to one of the defined categories.

Table 2
Categories of the inner surface quality and of the amplitude of wrinkling

| | 1 | 2 | 3 | 4 | 5 | 6 | 7 |
|---|---|---|---|---|---|---|---|
| Inner Surface Quality | Strong formation of dimpled skin | Weak formation of dimpled skin | Good surface quality | Weak formation of rills | Medium formation of rills | Strong formation of rills | - |
| Outer Surface Quality | Very good Surface Quality | Good Surface Quality | … | … | … | Bad Surface Quality | Very bad Surface quality |
| Amplitude of wrinkling | No | Weak | Inter-mediate | Strong | - | - | - |

Due to the variation of the spinning path in combination with the high variation of the feed-rate from $\kappa$ = 0,33 mm/min to $\kappa$ = 1 mm/min, the occurrence of wrinkling is amplified. But in order to produce a component with an optimal surface quality the process has to be pushed closely to the boundary region where wrinkling is likely to occur. This additionally points out the necessity to carry out a multivariate optimisation. Similar to the surface quality, wrinkling was assessed categorically because no reasonable method of measurement exists, see for example Kleiner et al. [27]. A scale of four categories was chosen with a smaller-the-better scale, see Table 2.

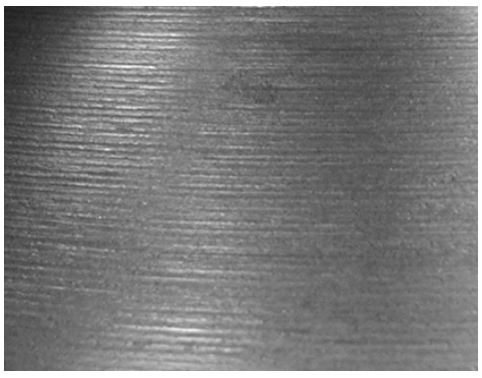

Fig. 7a. Rills caused by roller tool indentations

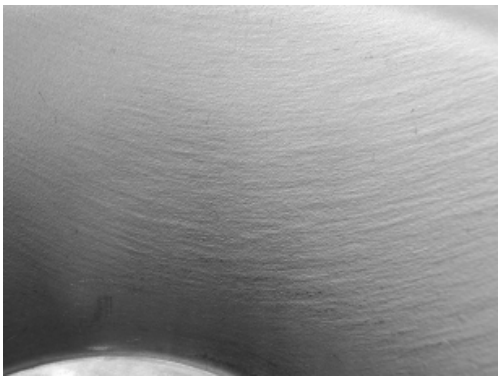

Fig. 7b. Dimpled skin due to forming process

### 3.3 Experimental design

For this study, a two-step procedure was applied to construct an appropriate mixed-level design with three two-level and two three-level factors. The basis of this design was a two-level fractional factorial $2^{7-2}$ design with 32 runs. In the first step, the method of replacement was used to substitute four two-level factors by two four-level factors. In the next step, the method of collapsing factors was used with a correspondence scheme yielding two three-level factors where the intermediate levels are observed twice as much as the extreme levels. With this design not only all main-effects of the factors are estimable, but also all important two-factor interactions. The mixed level design is shown in Table 1 in the Appendix. In order to assure the statistical properties the runs were made in randomised order. Additionally, after each sequence of eight runs a so-called null-run was made, where all factors except roller tool radius were set at their intermediate level, see Table 2 in the Appendix. By repeating this factor setting during the experiment, a possible time trend can easily be detected.

## 4. Results

### 4.1 Univariate models

Based on the theory of linear models, the effect estimates of the machine factors were calculated for each response variable. A hierarchical forward selection was used to identify the significant factors and interactions in the models. A significance level of 10% was used. In Table 4, all p-values of the statistical significant factors are given. The smaller the p-value the more important is the factor. The direction of influence is denoted by the algebraic sign, which is given in parentheses. A positive sign means that the response is increased with an increase of the value of the parameter while a negative sign indicates the opposite correlation. Values of the adjusted R-square, a measure of model fit, showed that each of the models described the relationship between the factors and the quality characteristics reasonably good.

Table 4
P-values of the significant factors (+ defines positive regression coefficients)

| | **Average wall thickness (target)** | **Cone angle (target)** | **Flange angle (target)** | **Inner surface quality (target)** | **Outer surface quality (minimal)** | **Amplitude of wrinkling (minimal)** |
|---|---|---|---|---|---|---|
| Roller tool radius | <0.01 (+) | <0.01 (+) | | <0.01 (-) | <0.01 (-) | <0.01 (+) |
| Roller tool feed | | | | <0.01 (+) | <0.01 (+) | |
| Revolution | | | | <0.01 (-) | 0.014 (-) | |
| Gap distance | <0.01 (+) | <0.01 (+) | <0.01 (-) | <0.01 (-) | <0.01 (-) | <0.01 (+) |
| Inclination of tool path | <0.01 (+) | <0.01 (+) | <0.01 (-) | | | |
| Radius * Gap distance | | | <0.01 (-) | <0.01 (+) | <0.01 (+) | |
| Radius * Inclination of tool path | | <0.01 (-) | | | | |
| Feed * Gap distance | | 0.025 (+) | | | | |
| Feed * Inclination of tool path | | | | 0.015 (+) | | |
| $(\text{Gap distance})^2$ | <0.01 (-) | 0.013 (+) | 0.064 (+) | <0.01 (-) | 0.014 (-) | |
| $(\text{Inclination of tool path})^2$ | 0.074 (-) | 0.087 (+) | | | | |

As can be seen, the influence of the machine factors on the responses is quite contradictory. For the two most important characteristics cone angel and surface quality, for example, the influence of the roller tool radius and the gap distance is reversed. Hence, to obtain a component with a good overall quality, compromises have to be found. In the next subsection the single characteristics are discussed in more detail, before in section 4.2 a multivariate optimization is carried out.

### 4.1.1 Surface quality at the in- and outside

The outer surface quality (category 1=very good surface quality, category 7=vary bad surface quality) is influenced by the process parameters nodes-radius of the roller tool, roller tool feed, revolution of the mandrel and the gap distance. Higher values of roller tool radius, revolution and gap distance result in a better surface quality on the outside. For the roller tool feed a reverse relationship is observed. These results mainly agree with the ones obtained by Chen et al. [20, 21], Murata and Ohara [18] and Hayama [16]. In this experiment, an important two-factor interaction between the roller tool radius and the gap distance could be observed. In order to interpret this effect a so-called interaction plot is helpful, see Figure 8.

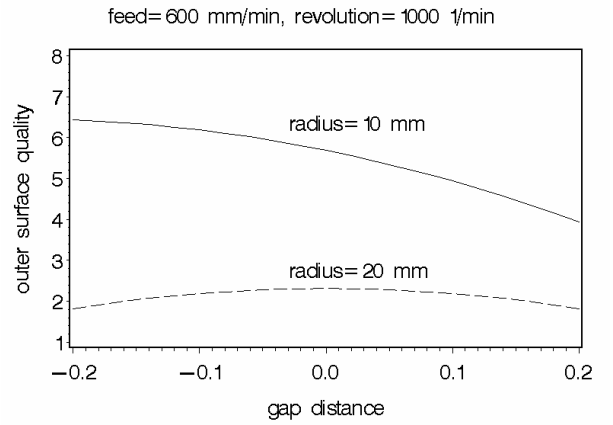


Fig. 8. Interaction of roller tool radius and gap distance for the outer surface quality

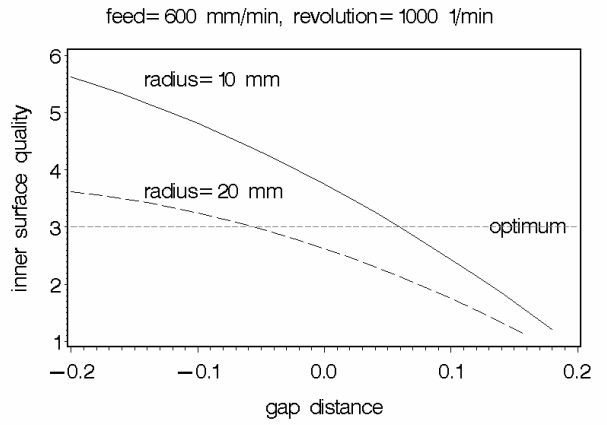


Fig. 9. Interaction of roller tool radius and gap distance for the inner surface quality

This plot graphically displays the interaction of the roller tool radius and the gap distance on the predicted outer surface quality, keeping the other machine factors fixed at their intermediate levels. Whereas for the roller tool with radius 10 mm the outer surface quality increases with increasing gap distance, for the roller tool with radius 20 mm the surface quality is mainly independent of the gap distance. The slightly curved form of the predicted functional relationship results from the significant quadratic effect of gap distance. This interaction is also observed by Chen et al. [21]. A possible explanation for the interaction is as follows, compare Figure 10. With a head-radius of 20 mm the single indentations of the roller tool can not be differentiated, hence, the surface is pretty smooth. But on the other hand the indentations caused by the roller tool with a radius of 10 mm can be separated. Smaller gap distances result in higher forces and consequently in deeper impacts, leading to a more pronounced formation of rills.

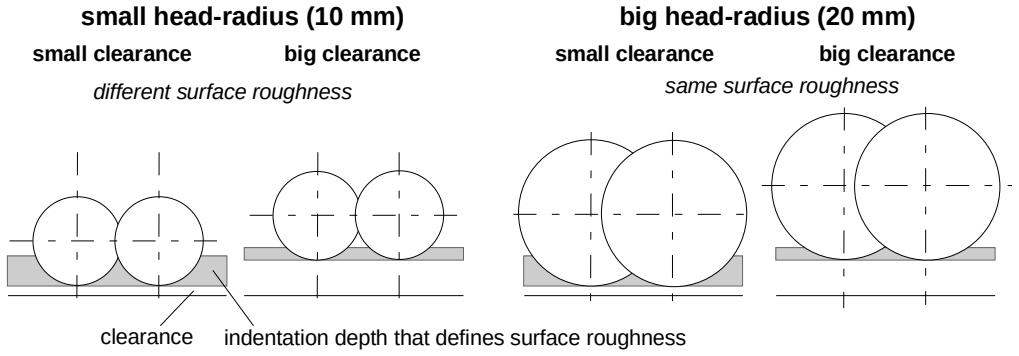


Fig. 10. Influence of the roller tool on surface quality

The surface quality on the inside is influenced by the same factors. Even the same interaction between the roller tool radius and the gap distance is observed. The interaction plot is shown in Figure 9. Interpretation of the coefficients is not as easy as for the outer surface quality, because deviations from the optimal category are considered in both directions. But we can say that higher values of the roller tool radius, mandrel revolution and gap distance lead to smaller predicted category numbers. In contrast, higher feed rates result in higher category numbers. Additionally, an interaction between feed and the inclination of tool path is observed.

### 4.1.2 Amplitude of wrinkling

The amplitude of wrinkling is a qualitative response variable with only four categories, where the fourth category of severe wrinkling was observed only three times out of 36. As a consequence, it is not reasonable to model the relationship between wrinkling and the machine factors by a regression model. A more appropriate model is the proportional odds model presented in section 2.3. As anticipated, the roller tool radius and the gap distance were identified to significantly influence the formation of wrinkling. Considering the positive algebraic sign, the formation of wrinkling is more likely to occur with a larger gap distance and a larger roller tool radius. While the fact that a larger gap distance increases the occurrence of wrinkling is well known from literature, an influence of the roller tool has not been observed before. But it has to be considered, that usually much smaller head-radii have been used, so that we here have significantly other conditions that could lead to other results.
Additionally, at a first glance it seems to be contradictory to the investigations of Murata and Ohara [18] and Hayama et al. [14] that the feed rate here could not be detected as influencing factor. But having a closer look to the results, is can be seen, that wrinkling at the experiments of Murata and Ohara [18] under comparable conditions usually occurs at feed rates of above 1.3 to 2 mm/rev. But here the feed rate is varied between 0.33 and 1 mm/rev., so that our result is not in contradiction to the other results. Also compared to the detailed theory of Hayama et al. [14] our process is completely within the stable region without wrinkling, see Fig 11. This Figure demonstrates the calculation of the theory for the HV-divider process. In the experiments of Hayama it is assumed, that the clearance is given by the sine law and head radii are smaller or equal than 10mm and a half apex angle is about 30°. This is similar to the process used here, so that the theory can be used. With a feed rate $\kappa = 0.33 \ldots 1$ mm/rev, a sheet thickness $t_0 = 2$ mm, flange height between $w(z) = 25 \ldots 80$ mm and workpiece radii between $r(z) = 50 \ldots 105$ mm the calculated region of the HV-divider process is clearly within the stable region. The grey coloured gap between wrinkling and no wrinkling takes variation of the fixed parameters into account.

### 4.1.3 Cone angle, flange angle and average wall thickness

The factors which significantly influence the responses describing the component geometry are mainly the same. These are roller tool radius, gap distance and inclination of the tool path. Higher values of these factors lead to higher values of the average wall thickness and cone angle. Instead, for the response flange angle, the influence of the gap distance and the inclination of tool path is reversed. For the cone angle a significant interaction between the roller tool radius and the inclination of tool path was identified. The interaction plot shows that for a smaller roller tool radius the influence of the inclination of the tool path is more pronounced, see Figure 12.

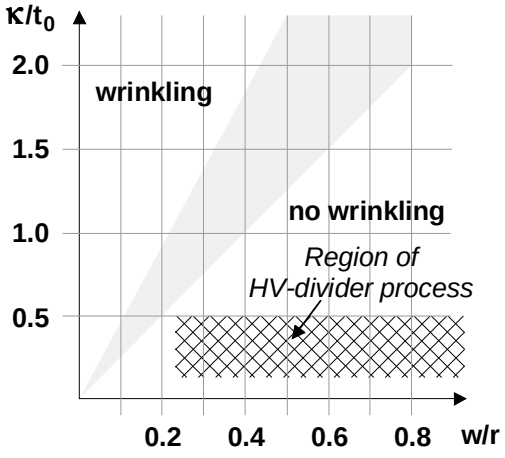


Fig. 11. HV-divider process in the theory of flange wrinkling of Hayama et al. [12].

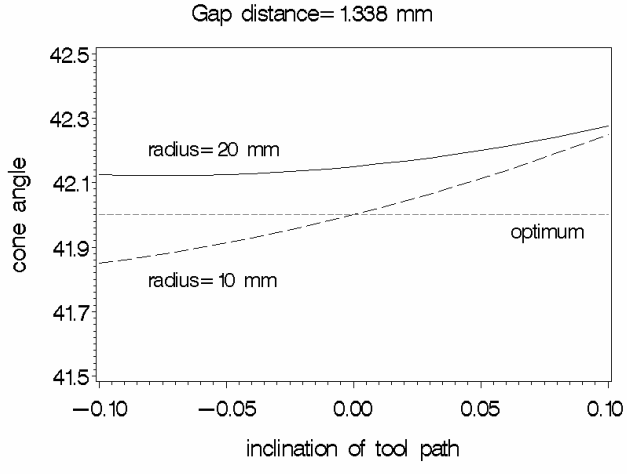


Fig. 12. Interaction between the tool radius and the inclination of the tool path for cone angle (gap distance fixed, according to the sine law)

It can be seen, that the target cone angle can be reached, according to the model, only with a head radius of 10 mm. In this case no inclination of the tool path is necessary and the process is according to the sine law. Additionally, a negative inclination of the tool path in a process with a head radius of 20 mm has no

effect on the cone angle. A second relevant interactions for the cone angle is observed for the feed and gap distance. For the flange angle, the radius and the gap distance seem to interact.
Comparing the significant factors for the responses describing the surface quality with those describing the geometry of the component, obvious differences exist. Whereas feed rate and mandrel revolution only influence the surface-quality responses, the tool path solely affects the workpiece geometry. Only the roller tool radius and the gap distance significantly influence all responses.

### 4.2 Multivariate optimisation

The goal of the experiments was to produce a component with very good surface quality and a closely followed geometry. Comparing the optimal parameter settings predicted by the univariate models quite contradictionary results are obtained for the individual responses, see Table 5. The differences are most pronounced among the two groups of responses describing the surface quality and the component geometry. Whereas, for example, for the inner and outer surface quality the roller tool with radius 20 mm is best, for the responses average wall-thickness and cone angle the roller tool with radius 10 mm is best. Hence, in order to find optimal parameter settings for the high voltage divider methods are needed which guarantee to find a reasonable compromise based on the requirements defined by the user.

Table 5
Predicted optimal parameter setting for the individual responses

| | **Tool radius** | **Tool feed** | **Revolution** | **Gap distance** | **Inclination of tool path** | **Prediction** | **Optimum** |
|---|---|---|---|---|---|---|---|
| Average wall thickness | 10 mm | | | 1.318 mm | 0 mm | 1.34 mm | 1.34 mm |
| Cone angle | 10 mm | | | 1.338 mm | 0 mm | 42° | 42° |
| Flange angle | 20 mm | | | 1.538 mm | 0.1 mm | 90.35° | 90° |
| Amplitude of Wrinkling | 10 mm | | | 1.138 mm | | 1 | 1 |
| Inner surface quality | 20 mm | 800 mm/min | 800 1/min | 1.378 mm | -0.08 mm | 3 | 3 |
| Outer surface quality | 20 mm | 400 mm/min | 1200 1/min | 1.138 mm | | 1 | 1 |

Applying the multivariate optimization approach presented in section 2.3, in the first step desirability functions have to be defined for each response. In Figure 13, the desirability functions for the surface quality responses are shown. For the surface quality on the inside, for example, a desirability of 1 is obtained for category 3. Figure 14 displays the desirability function of the cone angle.

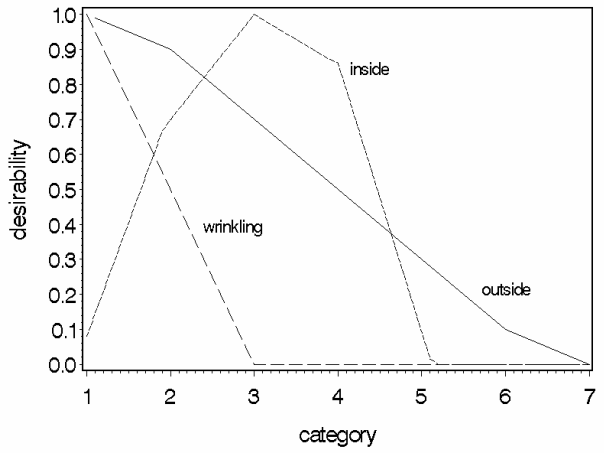


Fig. 13. Desirability functions for the amplitude of wrinkling and the inner and outer surface quality

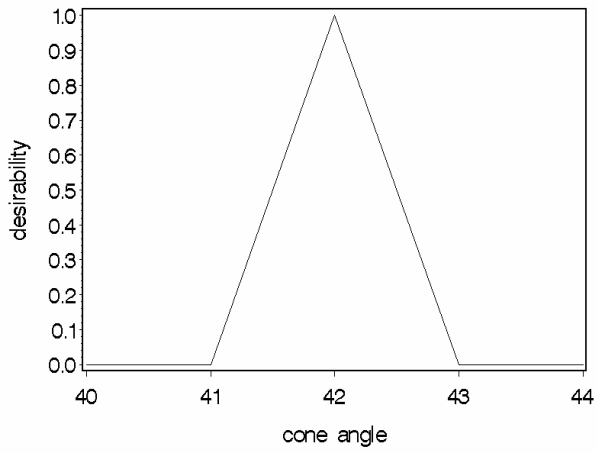


Fig. 14. Desirability function for the cone angle

For this response, deviations larger than one degree are not acceptable. Next to defining the desirability functions, a weighting of the individual responses is required. Since the goal in this study is to produce a high voltage divider with a very good surface quality the loading for the two corresponding responses was set higher than for the responses describing the workpiece geometry. The optimal parameter setting was calculated based on the overall desirability, see Table 6. The predicted values of the individual responses are given in Table 7. For this parameter setting an optimal surface quality is predicted (no amplitude of wrinkling, and a very good inner and outer surface quality). Also, for the predicted values of the responses describing the geometry of the component quite good predictions are made. Among these responses, the one yielding the smallest desirability is the flange angle.

Table 6
Optimal parameter setting

| Tool radius | Tool feed | Revolution | Gap distance | Inclination of tool path |
|---|---|---|---|---|
| 20 mm | 400 mm/min | 1160 1/min | 1.318 mm | -0.1 mm |

To validate the approach, three components with this optimal setting of the machine parameters were produced. For each of the responses, the arithmetic mean of the three runs is shown in Table 7. The observed values are quite close to the predicted values.
The adequacy of the models is checked by calculating the 95 per cent prediction intervals. Obviously, the prediction adequacy for all models could be verified. Only for the outer surface quality does the observed value narrowly fall outside the predicted interval. But a deviation from 0.46 between the predicted and observed value is acceptable since the regression model predicts continuously between the categories and in praxis only integers are observed.

Table 7
Predicted values of the responses and their confidence limits for the optimal parameter setting

| | Average wall thickness | Cone angle | Flange angle | Inner surface quality | Outer surface quality | Amplitude of wrinkling |
|---|---|---|---|---|---|---|
| Prediction | 1.361 mm | 42.09° | 7.1° | 2.76 | 1.46 | 1 |
| Observed | 1.35 mm | 42.11° | 7.04° | 3 | 1 | 1 |
| Lower confidence limit (95%) | 1.339 mm | 41.99° | 5.24° | 2.29 | 1.08 | |
| Upper confidence limit (95%) | 1.383 mm | 42.17° | 9.25° | 3.22 | 1.83 | |

For the spun components of the design, overall desirabilities between 0 and 0.745 are observed, see Figure 15. The mean value is 0.3718. For the optimal component an overall desirability of 0.885 was observed. Hence, compared to the best spun component from the 32 experiments, an additional improvement of more than 20 per cent could be gained.

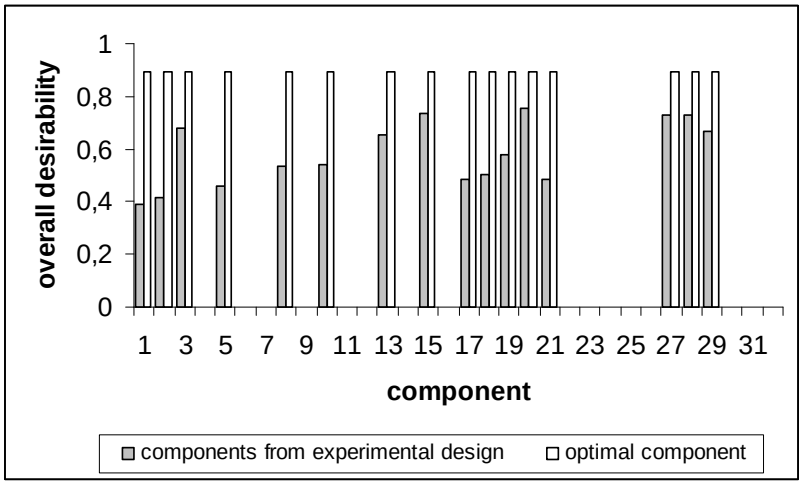


Fig. 15: Comparison of overall desirabilities

Next to the fact that with the multivariate approach the best reasonable compromise between the contradictionary responses could be found, a further important advantage of this approach exists. If the demands for a component with a special geometry change, then it is not necessary to conduct new experiments to identify the new optimal parameter setting. Since the univariate models remain valid, it is only necessary to specify a new weighting and possibly modify the desirability functions. The new optimal parameter setting can then easily be calculated based on the overall desirabilities. Hence, this multivariate optimisation approach is an effective and efficient tool for optimisation of several contradictionary responses.

## 5. Summary

Based on the experiments performed, a high voltage divider with very good surface qualities and nearly exact workpiece geometries could be produced. In the first step, the most important machine factors were identified. Next to classical machine factors like roller tool radius, roller tool feed, and mandrel revolution, the gap distance and the inclination of the roller tool path were considered. In order to assess the geometry of the component, the cone and flange angle and the wall-thickness were measured. As indicators for the surface quality, the inner and outer surface quality and the amplitude of wrinkling were observed. For the surface quality on the inside, it was differentiated between the formation of rills and dimpled skin.
For each of the responses, a mathematical model could be fitted which describes the influence of the machine factors reasonably well. Significant interactions could be identified and interpreted.
A multivariate optimisation method based on the concept of desirabilities allowed to identify a parameter setting of best compromise between the mutually contradictionary quality characteristics. Producing a high voltage divider with this parameter setting resulted in an optimal component. An additional advantage of this multivariate optimization approach is the flexibility with respect to customer requirements. This approach allows optimising components for varying demands of the customers without the need to perform new experiments.
The statistical methods described in this paper are easy to use and to implement. The proposed multivariate optimisation procedure is applicable to any process.

## Acknowledgement

Financial support by the Deutsche Forschungsgemeinschaft (SFB 475 - Reduction of Complexity in Multivariate Data Structures) is gratefully acknowledged. Special thanks to the company Poynting GmbH, Dortmund, Germany for the close and excellent co-operation.

## References

[1] Ott Metalldrückerei AG, Affeltrangen, Switzerland. www.ottmetall.ch
[2] C.C. Wong, T.A. Dean, J. Lin, A review of spinning, shear forming and flow forming processes, International Journal of Machine Tools and Manufacture 43 (2003) 1419-1435.
[3] G.T. Smith, Go with the flow! An Appraisal of CNC Spinning and Shear Forming Techniques, Proceedings of the International Conference of Sheet Metal 1992, The Birmingham Polytechnic, Birmingham, Great Britain, 1992, 417 – 428.
[4] S. Kalpakcioglu, On the mechanics of shear spinning, Transactions of the ASME, Journal of Engineering for Industry 83 (1961) 125-130.
[5] B. Avitzur, Handbook of Metal-Forming Processes, John Wiley and Sons, Inc., Canada, 1983.
[6] B. Avitzur, C.T. Yang, Analysis of power spinning of cones, Transactions of the ASME, Journal of Engineering for Industry 82 (1960) 231-245.
[7] S. Kobayashi, I.K. Hall, E.G. Thomsen, A theory of shear spinning of cones, Transactions of the ASME, Journal of Engineering for Industry 81 (1961) 485-495.
[8] S. Kobayashi, Instability in the conventional spinning of cones, Transactions of the ASME, Journal of Engineering for Industry 85 (1963), 44-48.
[9] R.A.C. Slater, A. Joorabchian, Spinforging of sheet metal cones having various cone angles and an upper bound estimate for the tangential component force exerted at the workpiece roller

interface, Proceedings of the 17th International MTDR Conference, University of Birmingham, 1976, 521-529.
[10] M. Hayama, Analysis of Working Force in Shear Spinning of Cones, Bulletin of the Faculty of Engineering, Yokohama National University, Vol 26, March, 1977, 99-116.
[11] M. Hayama, Study on the Spinnability of Aluminum and it's Alloys, Proceeding of the 1st International Conference on Rotary Metal-Working Processes, London, UK, November 20-22, 1979, 207 – 216.
[12] G. Dan, Z. Zheng, F. Chu, Vibration analysis of spinning cylindrical shells by finite element method. International Journal of Solids and Structures 39 (2002), 3, 725-739.
[13] C. Kim, S.Y. Jung, J.C. Choi, A lower upper-bound solution for shear spinning of cones, International Journal of Mechanical Sciences 45 (2003), 11, 1893-1911.
[14] M. Hayama, T. Murota, H. Kudo, Experimental Study of Shear Spinning, Bulletin of JSME 8/31 (1965) 453 – 460.
[15] M. Hayama, T. Murota, H. Kudo, Deformation Modes and Wrinkling of Flange on Shear Spinning, Bulletin of JSME 9/31 (1966) 423-433.
[16] M. Hayama, A. Tago, The Fracture of Walls on Shear Spinning, Bulletin of the Faculty of Engineering, Yokohama National University, Vol. 17, March, 1968, 93-103.
[17] M. Hayama, Study of Lubrication in Shear Spinning, Bulletin of the Faculty of Engineering, Yokohama National Univ. Vol 20, March, 1971, 61-69.
[18] M. Murata, N. Ohara, Truncated Cone Spinning of Sheet Metal, Proceedings of the 9th International Conference on Sheet Metal (2001), Leuven, Belgium, 199-204.
[19] R.A.C. Slater, A. Joorabchian, An experimental study of the spin-forging of sheet metal cones using a mandrel of constant cone angle, 17th International MTDR Conference, University of Birmingham, 1976, 531-537.
[20] M.D. Chen, R.Q. Hsu, K.H Fuh, Forecast of shear spinning force and surface roughness of spun cones by employing regression analysis, International Journal of Machine Tools and Manufacture 41 (2001) 1721-1734.
[21] M.D.Chen, R.Q. Hsu, K.H. Fuh, Effects of over-roll thickness on cone surface roughness in shear spinning, Journal of materials processing technology, 159 (2005), 1, 1-8.
[22] D.C. Montgomery, Design and Analysis of Experiments, John Wiley and Sons, Inc., Canada, 1997.
[23] S. Addelman, Orthogonal main-effects plans for asymmetrical factorial experiments, Technometrics 4 (1962) 21-46.
[24] S. Addelman, Symmetrical and asymmetrical fractional factorial plans, Technometrics 4 (1962) 47-58.
[25] A. Agresti, Categorical data analysis, John Wiley and Sons, New York, 1990.
[26] G. Derringer, R. Suich, Simultaneous optimization of several response variables, Journal of Quality Technology 12 (1980) 214-219.
[27] M. Kleiner, R. Göbel, H. Kantz, Ch. Klimmek, W. Homberg, Combined Methods for the Prediction of Dynamic Instabilities in Sheet Metal Spinning, Annals of the CIRP 51/1 (2002) 209-214.

**Appendix**

Table 1
Mixed level design with 32 runs

| Run | Tool radius | Tool feed | Mandrel revolution | Gap distance | Inclination of roller path |
|---|---|---|---|---|---|
| 1 | 10 mm | 400 mm/min | 800 1/min | 1.138 mm | 0.1 mm |
| 2 | 20 mm | 400 mm/min | 800 1/min | 1.138 mm | -0.1 mm |
| 3 | 10 mm | 800 mm/min | 800 1/min | 1.138 mm | -0.1 mm |
| 4 | 20 mm | 800 mm/min | 800 1/min | 1.138 mm | 0.1 mm |
| 5 | 10 mm | 400 mm/min | 1200 1/min | 1.138 mm | 0.0 mm |
| 6 | 20 mm | 400 mm/min | 1200 1/min | 1.138 mm | 0.0 mm |
| 7 | 10 mm | 800 mm/min | 1200 1/min | 1.138 mm | 0.0 mm |
| 8 | 20 mm | 800 mm/min | 1200 1/min | 1.138 mm | 0.0 mm |
| 9 | 10 mm | 400 mm/min | 800 1/min | 1.338 mm | -0.1 mm |
| 10 | 20 mm | 400 mm/min | 800 1/min | 1.338 mm | 0.1 mm |
| 11 | 10 mm | 800 mm/min | 800 1/min | 1.338 mm | 0.1 mm |
| 12 | 20 mm | 800 mm/min | 800 1/min | 1.338 mm | -0.1 mm |
| 13 | 10 mm | 400 mm/min | 1200 1/min | 1.338 mm | 0.0 mm |
| 14 | 20 mm | 400 mm/min | 1200 1/min | 1.338 mm | 0.0 mm |
| 15 | 10 mm | 800 mm/min | 1200 1/min | 1.338 mm | 0.0 mm |
| 16 | 20 mm | 800 mm/min | 1200 1/min | 1.338 mm | 0.0 mm |
| 17 | 10 mm | 400 mm/min | 800 1/min | 1.338 mm | 0.0 mm |
| 18 | 20 mm | 400 mm/min | 800 1/min | 1.338 mm | 0.0 mm |
| 19 | 10 mm | 800 mm/min | 800 1/min | 1.338 mm | 0.0 mm |
| 20 | 20 mm | 800 mm/min | 800 1/min | 1.338 mm | 0.0 mm |
| 21 | 10 mm | 400 mm/min | 1200 1/min | 1.338 mm | -0.1 mm |
| 22 | 20 mm | 400 mm/min | 1200 1/min | 1.338 mm | 0.1 mm |
| 23 | 10 mm | 800 mm/min | 1200 1/min | 1.338 mm | 0.1 mm |
| 24 | 20 mm | 800 mm/min | 1200 1/min | 1.538 mm | -0.1 mm |
| 25 | 10 mm | 400 mm/min | 800 1/min | 1.538 mm | 0.0 mm |
| 26 | 20 mm | 400 mm/min | 800 1/min | 1.538 mm | 0.0 mm |
| 27 | 10 mm | 800 mm/min | 800 1/min | 1.538 mm | 0.0 mm |
| 28 | 20 mm | 800 mm/min | 800 1/min | 1.538 mm | 0.0 mm |
| 29 | 10 mm | 400 mm/min | 1200 1/min | 1.538 mm | 0.1 mm |
| 30 | 20 mm | 400 mm/min | 1200 1/min | 1.538 mm | -0.1 mm |
| 31 | 10 mm | 800 mm/min | 1200 1/min | 1.538 mm | -0.1 mm |
| 32 | 20 mm | 800 mm/min | 1200 1/min | 1.538 mm | 0.1 mm |

Table 3
Results of the mixed-level design

| Run | Average wall thickness | Cone angle | Flange angel | Inner surface quality | Outer surface quality | Amplitude of wrinkling |
|---|---|---|---|---|---|---|
| 1 | 1,23 mm | 41,9° | -11,3° | 5 | 5 | 1 |
| 2 | 1,40 mm | 42,3° | -2,9° | 1 | 4 | 2 |
| 3 | 1,29 mm | 41,9° | -7,3° | 4 | 5 | 1 |
| 4 | 1,31 mm | 42,0° | -3,9° | 4 | 7 | 1 |
| 5 | 1,33 mm | 42,1° | -4,0° | 5 | 5 | 1 |
| 6 | 1,24 mm | 41,8° | -4,1° | 6 | 7 | 1 |
| 7 | 1,27 mm | 42,0° | -8,6° | 4 | 7 | 1 |
| 8 | 1,26 mm | 41,9° | -8,4° | 4 | 6 | 1 |
| 9 | 1,27 mm | 42,1° | 24,8° | 3 | 2 | 2 |
| 10 | 1,26 mm | 42,0° | -14,3° | 3 | 2 | 2 |

| | | | | | | |
|---|---|---|---|---|---|---|
| 11 | 1,41 mm | 42,1° | -3,6° | 4 | 3 | 3 |
| 12 | 1,45 mm | 42,3° | 2,1° | 2 | 2 | 3 |
| 13 | 1,38 mm | 42,1° | 9,9° | 4 | 3 | 2 |
| 14 | 1,41 mm | 42,1° | 6,5° | 3 | 2 | 3 |
| 15 | 1,36 mm | 42,2° | 7,0° | 3 | 2 | 2 |
| 16 | 1,39 mm | 42,2° | 5,8° | 2 | 2 | 3 |
| 17 | 1,40 mm | 42,2° | -3,5° | 1 | 4 | 1 |
| 18 | 1,40 mm | 42,1° | -2,8° | 1 | 4 | 1 |
| 19 | 1,34 mm | 42,0° | -5,8° | 4 | 6 | 1 |
| 20 | 1,37 mm | 42,0° | -4,2° | 3 | 5 | 1 |
| 21 | 1,39 mm | 42,4° | -3,5° | 1 | 3 | 1 |
| 22 | 1,35 mm | 42,2° | -0,1° | 5 | 6 | 4 |
| 23 | 1,27 mm | 42,5° | -8,9° | 6 | 6 | 1 |
| 24 | 1,13 mm | 41,7° | -9,1° | 6 | 7 | 1 |
| 25 | 1,45 mm | 42,4° | 2,0° | 1 | 2 | 3 |
| 26 | 1,45 mm | 42,3° | 3,5° | 1 | 2 | 3 |
| 27 | 1,34 mm | 42,3° | 2,1° | 2 | 1 | 2 |
| 28 | 1,42 mm | 42,2° | 2,9° | 2 | 2 | 2 |
| 29 | 1,22 mm | 42,0° | -13,8° | 4 | 1 | 1 |
| 30 | 1,30 mm | 42,1° | -9,4° | 6 | 3 | 1 |
| 31 | 1,43 mm | 42,5° | 1,6° | 1 | 2 | 3 |
| 32 | 1,44 mm | 42,5° | -1,7° | 1 | 2 | 4 |